SUPRATHERMAL X-RAY EMISSIVITY WITH 2ND AND 3RD HARMONIC ELECTRON CYCLOTRON HEATING IN THE TCV TOKAMAK

S. Coda, Y. Peysson[a], S. Alberti, T.P. Goodman, M.A. Henderson, P. Nikkola, O. Sauter

Centre de Recherches en Physique des Plasmas
Association EURATOM-Confédération Suisse
Ecole Polytechnique Fédérale de Lausanne, CH-1015 Lausanne, Switzerland

[a]*Département de Recherches sur la Fusion Contrôlée, Association EURATOM-CEA, CEA/Cadarache, 13108 Saint Paul-lez-Durance Cédex, France*

1. Introduction

A multichordal, multichannel hard X-ray (HXR) pinhole camera, on loan from Tore Supra, is used on the TCV tokamak to study the spatial and spectral distribution of bremsstrahlung emission in the 10-200 keV range. Photon detection is effected by a linear array of CdTe detectors [1] with an intrinsic energy resolution of ~7 keV. Eight energy channels, with adjustable thresholds, are available for each of 14 vertical viewing chords, which span the outboard half of the plasma cross section with partially overlapping étendues and a radial resolution of approximately 2 cm on the midplane (see Fig. 1).

Hard X-ray radiation in the energy range under consideration is emitted by suprathermal electrons, and can thus be used to diagnose their spatial distribution and temporal dynamics; indirect information on the energy distribution of the fast electron population can also be gleaned from the HXR spectrum. In TCV, substantial HXR emission is generated when high power electron cyclotron waves are injected in the plasma with a finite parallel wave number; this injection scheme, which is used for electron cyclotron current drive (ECCD), creates measurable non-thermal photon distributions for injection angles deviating by more than 4-5^{o} from the normal to the magnetic field [2]. For smaller angles, when the applied power is sufficient to raise the electron temperature above ~4 keV, the HXR diagnostic detects only the emission from the tail of the bulk Maxwellian distribution.

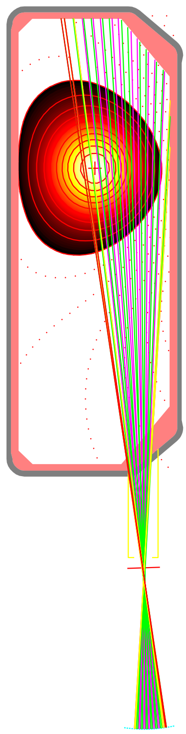

Fig. 1 *Geometry of hard X-ray camera. The chords are partially overlapped.*

The results presented in this paper pertain to the first set of experiments carried out with 470 kW third harmonic X-mode (X3) electron cyclotron heating (ECH) at 118 GHz [3]. The power was applied through a lateral launcher to the plasma center after a second harmonic X-mode (X2) preheating phase. The target plasmas has major radius R=0.88 m, minor radius a=0.25 m, elongation κ=1.31, magnetic field B_T=1.42 T and central density $n_{e0}=2.5\times10^{19}$ m^{-3}. The X2 and X3 cold resonance locations are separated by ~5 cm and are distributed symmetrically on the high and low field sides of the magnetic axis, respectively. Both the X2 and X3 waves are launched from the low field side of the torus. The X2 power and launching geometry, as well as the plasma current, were selectively varied over a set of discharges in order to characterize the X3 absorption efficiency under a variety of conditions.

2. Dependence of suprathermal emission on X2 injection angle

The primary result of the X2-X3 experiments is that the absorbed X3 power fraction, measured by a diamagnetic loop (DML), is larger than the value predicted by linear calculations based on a Maxwellian distribution function [3]. In particular, a scan of the X2 toroidal injection angle, for constant 200 kA current and 470 kW X2 power, has revealed that the absorption has two maxima at $\phi\sim\pm20^o$ (where ϕ=-arcsin[**k·B/(**kB)] at the absorption location, **k** is the wave vector, and the sign of ϕ is positive for co-current drive). The two peaks are asymmetric, the positive one being larger and reaching ~100%.

The HXR energy channels in this experiment were set at 8 keV intervals from 8 to 64 keV. In general, the logarithms of the spectra reveal the presence of two features: a low energy component with a slope consistent with the bulk temperature, and a higher energy component with lower amplitude but a lesser slope. By excluding the first two energy channels, a satisfactory linear fit can generally be obtained for the suprathermal part; the fit is robust in that the resulting photon temperature is insensitive to the elimination of additional channels. The result of the fit can be written as $d\gamma/dE=Ae^{-E/T}$, where γ is the emissivity; we can then characterize the suprathermal population by the temperature T_{ph} and the total emissivity $\gamma_{tot}=AT_{ph}$ for a central chord, i.e. for emissivity line-integrated over the entire plasma cross section. These two parameters are shown in Fig. 2 as functions of ϕ, for both the preheating X2 phase and the combined X2-X3 phase; the X3 absorbed power fraction is also plotted for comparison. The HXR signal was integrated over 0.2 s. The photon temperature during X2 heating increases indefinitely with |ϕ|, confirming earlier results [2]; by contrast, the total emissivity peaks at the angles

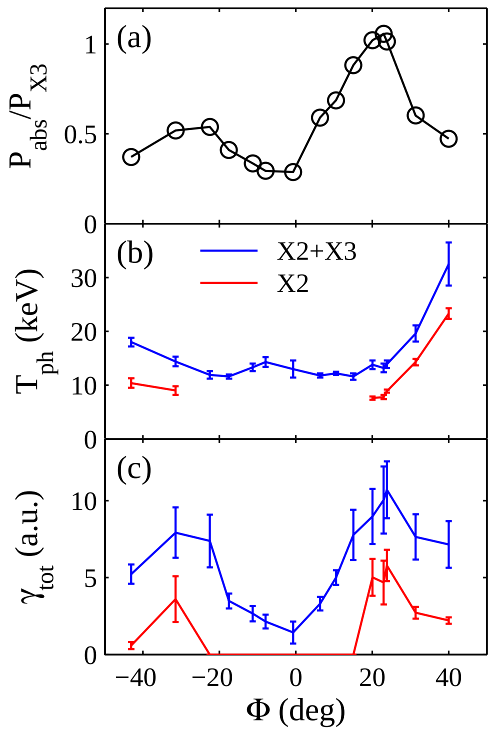

Fig. 2 *(a) X3 absorbed power fraction, (b) HXR suprathermal photon temperature, (c) integrated HXR emissivity, vs. ϕ (complementary to the angle between X2 wave vector and magnetic field). The suppressed points correspond to cases in which only the thermal spectrum is measurable.*

for which the X3 absorption is maximized. When X3 is applied, the emissivity increases further in all cases and the dependence on ϕ remains qualitatively similar. The photon temperature during X2+X3 is approximately 12-14 keV with little dependence on ϕ except at the highest angles, where an increase with $|\phi|$ is observed.

These results strongly suggest that the anomalously high absorption efficiency of X3 ECH is related to the presence of a suprathermal electron population in the plasma, which lies outside the scope of linear calculations in ray tracing codes. The further acceleration of these fast electrons by the X3 waves leads to a further increase in the emissivity. The final photon temperature, and indeed the form of the HXR spectra on all the chords, are only weakly dependent on ϕ. This suggests that the intrinsic efficiency of X3 absorption by the fast electron population is relatively insensitive to the detailed spectrum of the initial “seed” distribution, and that the ultimate distribution is primarily determined by the characteristics of the X3 waves. Only for the highest toroidal angles, at which the X2 waves are able to significantly populate energy levels in excess of 50 keV, does the final distribution retain a measurable memory of the seed distribution. The most significant factor influencing the X3 absorption thus appears to be the total density of fast electrons rather than their energy distribution.

3. Spatial distribution of hard X-ray emissivity

The spatial distribution of the local HXR emissivity is reconstructed by assuming poloidal homogeneity and performing profile inversions with the Fischer regularization method. The spatial profiles, normalized to a maximum of unity, are shown for both the X2 and X2+X3 phases for several values of ϕ in Fig. 3. The 40-48 keV energy range has been chosen to prevent pollution of the signal by the thermal bulk. The location of the primary peak can be taken to be at ρ=0 in all cases, as the shift to ρ~0.1 seen in some discharges is not significant within the accuracy of the equilibrium reconstruction (ρ is the square root of the normalized poloidal flux). The width of the X2 profiles is an increasing function of $|\phi|$, consistent with the

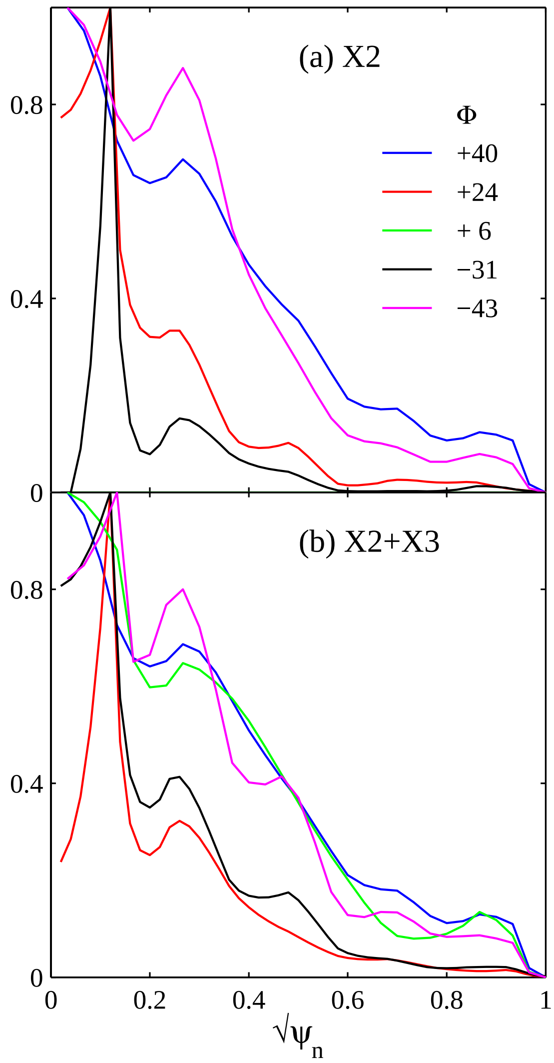

Fig. 3 *Profiles of local HXR emissivity in the 40-48 keV range for (a) X2 and (b) combined X2 and X3 heating, vs. normalized radial coordinate, for 5 values of the angle* ϕ*.*

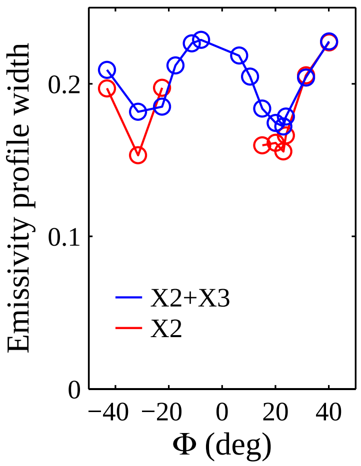

Fig. 4 *Root mean square width (in units of $\psi_n^{-1/2}$) of the HXR emissivity profile, in the X2 and X2+X3 heating phases, vs. X2 resonance angle* ϕ.

increasing spread of the absorption region towards the low field side caused by Doppler shift of the resonance frequency. The X2+X3 profiles are close to their X2 counterparts for angles at which there is a measurable suprathermal signal during X2; at lower values of $|\phi|$, the X2+X3 profiles become broader and essentially independent of ϕ. This is exemplified by Fig. 4, which shows the rms profile width as a function of ϕ. It may be speculated that X3 absorption, and the attendant fast electron acceleration, occurs preferentially in the spatial region occupied by the seed suprathermal electrons; at the smallest angles, for which the seed population is negligible, the X3 absorption coefficient is smaller and the damping profile appears to be determined by the properties of the X3 wave alone.

In spite of the strong variation of the absolute emissivity across the plasma cross section, the form of the spectrum is essentially constant in space, as illustrated in Fig. 5 by the spatial distribution of the photon temperature. This is true in a wide variety of conditions and suggests that the radial diffusion rate of suprathermal electrons may not depend significantly on energy.

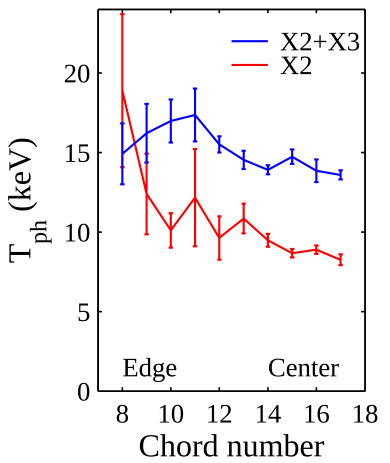

Fig. 5 *Suprathermal photon temperature from line-integrated HXR emission vs. chord number, in the X2 and X2+X3 phases of a shot with* $\phi=+24^o$.

Acknowledgments

The loan of the HXR camera and associated electronics by the CEA is gratefully acknowledged. Thanks are due to L. Delpech for technical support and to the entire TCV team for the operation of the tokamak and of the auxiliary heating systems. This work was supported in part by the Swiss National Science Foundation.

References

[1] Y. Peysson, S. Coda and F. Imbeaux, Nucl. Instrum. and Methods in Phys. Res. A **458** (2001) 269; Y. Peysson and F. Imbeaux, Rev. Sci. Instrum. **380** (1999) 3987.

[2] S. Coda et al., Proc. 26th EPS Conf. on Controlled Fusion and Plasma Physics (Maastricht 1999), Europhys. Conf. Abstr. **23J** (1999) 1097.

[3] S. Alberti et al., Proc. 18th Int. Conf. on Plasma Physics and Controlled Nuclear Fusion Research, Sorrento, Italy, 2000 (IAEA, Vienna, to be published).

[4] R.W. Harvey and M.G.McCoy, in Proc. IAEA TCM/Advances in Simulation and Modeling in Thermonuclear Plasmas, Montreal (1992)